

## Semi-discretization method for delayed systems

Tamás Insperger<sup>‡</sup> and Gábor Stépán<sup>\*,†</sup>

*Department of Applied Mechanics, Budapest University of Technology and Economics,  
Budapest H-1521, Hungary*

### SUMMARY

The paper presents an efficient numerical method for the stability analysis of linear delayed systems. The method is based on a special kind of discretization technique with respect to the past effect only. The resulting approximate system is delayed and also time periodic, but still, it can be transformed analytically into a high-dimensional linear discrete system. The method is applied to determine the stability charts of the Mathieu equation with continuous time delay. Copyright © 2002 John Wiley & Sons, Ltd.

KEY WORDS: time delay; periodic system; Floquet theory; linear stability

### 1. INTRODUCTION

There are several mechanical models which lead to equations of motion governed by delayed-differential equations (DDEs). In mechanical engineering, for example, the models describing the regenerative effect in machine tool vibrations [1], the human/machine systems involving the human operator's reflex delay, or the robotics applications like telemanipulation with information delay can be mentioned [2]. The corresponding mechanical models are often low degree-of-freedom (DOF) oscillatory systems subjected to the delayed feed-back of the state variables. The stability analysis of these systems is an important and crucial problem.

The advanced mechanical models include parametric excitation, too. In case of a human operator, the reflex delay can vary in time; in case of machining, the cutting speed [3], or the number of active teeth [4] can change periodically; while in the case of telemanipulation, a time-varying parameter may help to compensate the destabilizing effect of large time delays [5]. Problems like these require the stability analysis of linear, time-periodic delayed oscillatory systems, described by linear non-autonomous DDEs.

---

\*Correspondence to: G. Stépán, Department of Applied Mechanics, Budapest University of Technology and Economics, Budapest H-1521, Hungary.

<sup>†</sup>E-mail: [stepan@mm.bme.hu](mailto:stepan@mm.bme.hu)

<sup>‡</sup>E-mail: [inspi@mm.bme.hu](mailto:inspi@mm.bme.hu)

Contract/grant sponsor: Hungarian National Science Foundation; contract/grant number: OTKA T030762/99

Contract/grant sponsor: COST Action P4

According to the well-known theory of linear autonomous ordinary differential equations (ODEs), the stability properties are determined by the roots of the characteristic polynomial: if and only if all the characteristic roots have negative real parts, the system is asymptotically stable. The famous Routh–Hurwitz criterion provides an algorithm to check this condition in characteristic polynomials [6, 7].

The phenomenon of parametric excitation was observed already in the 19th century. The theory of periodic systems was outlined by Floquet [8]. The general form of an  $n$ -dimensional linear  $T$ -periodic system reads

$$\dot{\mathbf{y}}(t) = \mathbf{A}(t)\mathbf{y}(t), \quad \mathbf{A}(t) = \mathbf{A}(t + T) \quad (1)$$

All the solutions have the form  $\mathbf{y}(t) = \mathbf{\Phi}(t)\mathbf{y}(0)$ , where  $\mathbf{\Phi}(t)$  is the so-called fundamental matrix of system (1). The matrix  $\mathbf{\Phi}(T)$  is the so-called principal or transition matrix, its eigenvalues are the characteristic multipliers calculated from

$$\det(\mu\mathbf{I} - \mathbf{\Phi}(T)) = 0 \quad (2)$$

The trivial solution  $\mathbf{y}(t) \equiv 0$  of system (1) is asymptotically stable, if and only if all the characteristic multipliers are in modulus less than one. Generally, this condition is hard to apply, since there is no closed-form representation for the principal matrix. For practical applications, approximate methods are used, see e.g. References [9–12]. The basic stability chart of periodic systems, the Strutt–Ince diagram of Mathieu equation was first published by van der Pol and Strutt [13].

Linear autonomous DDEs have the general form

$$\dot{\mathbf{y}}(t) = \mathbf{L}(\mathbf{y}_t), \quad \mathbf{L}(\mathbf{y}_t) = \int_{-\sigma}^0 d\boldsymbol{\eta}(\vartheta)\mathbf{y}(t + \vartheta) \quad (3)$$

where the matrix  $\boldsymbol{\eta}$  is a function of bounded variation on  $[-\sigma, 0]$  and the integral is a Stieltjes one, i.e. it describes discrete and continuous time delays as well. The linear functional  $\mathbf{L}$  can be represented in the above matrix form according to the Riesz representation theorem [14], and the continuous function  $\mathbf{y}_t$  is defined by the shift

$$\mathbf{y}_t(\vartheta) = \mathbf{y}(t + \vartheta), \quad \vartheta \in [-\sigma, 0] \quad (4)$$

The characteristic function of system (3) reads

$$\det \left( \lambda\mathbf{I} - \int_{-\sigma}^0 e^{\lambda\vartheta} d\boldsymbol{\eta}(\vartheta) \right) = 0 \quad (5)$$

Opposite to the characteristic polynomial of autonomous ODEs, this characteristic function has, in general, infinite number of zeros. The books of Hale [14], Hale and Lunel [15] and Diekmann *et al.* [16] summarize the most important theorems for DDEs. The sufficient and necessary condition for asymptotic stability of Equation (3) is that all the infinite number of characteristic roots have negative real parts.

The first attempts for determining stability criteria for second-order DDEs was made by Bellmann and Cooke [17] and by Bhatt and Hsu [18]. They used the D-subdivision method [19]

combined with a theorem of Pontryagin [20]. The book of Kolmanovskii and Nosov [21] summarizes the main theorems on stability of DDEs, and it contains several examples as well. A more sophisticated method was developed by Stépán [2] (generalized also by Hassard [22]) applicable even for the combination of several discrete and continuous time delays.

Linear periodic DDEs have the general form

$$\dot{\mathbf{y}}(t) = \mathbf{L}(t, \mathbf{y}_t), \quad \mathbf{L}(t, \mathbf{y}_t) = \int_{-\sigma}^0 d_\vartheta \boldsymbol{\eta}(t, \vartheta) \mathbf{y}(t + \vartheta), \quad \mathbf{L}(t + T, \mathbf{y}_t) = \mathbf{L}(t, \mathbf{y}_t) \quad (6)$$

The Floquet theorem can be extended for these systems [23], but infinite-dimensional linear operators are used instead of the finite-dimensional tensors in (2). Such a linear operator can be defined by  $\mathbf{y}_t = \mathbf{U}(t)\mathbf{y}_0$ . While  $\mathbf{U}(t)$  plays the role of the fundamental matrix, the role of the principal matrix is taken by  $\mathbf{U}(T)$ . The non-zero elements of the spectrum of  $\mathbf{U}(T)$  are called the characteristic multipliers of system (6), also defined by

$$\text{Ker}(\mu \mathbf{I} - \mathbf{U}(T)) \neq \emptyset \quad (7)$$

instead of (2).

For periodic DDEs, the difficulty is that the operator  $\mathbf{U}(t)$  has no closed form, so no stability conditions can be expected in closed form either. For practical calculations, only approximations can be applied. Stability investigations are often carried out by numerical simulations, see e.g. Balachandran's simulations for milling processes [24]. A low-dimensional discrete map approximation was used by Davies *et al.* [25] and Bayly *et al.* [26] for stability analysis of interrupted cutting. Another approach was developed by Insperger and Stépán [4] for milling process analysis, when the discrete time delay is approximated by special continuous ones, and the infinite-dimensional eigenvalue problem is transformed into an approximate finite-dimensional one. An alternative of Hill's method was used by Seagalman and Butcher [27] to determine stability properties of turning process with harmonic impedance modulation. Insperger and Stépán [28] also used Hill's method to determine the closed-form stability chart for the Mathieu equation with one discrete delay.

The semi-discretization method was composed and applied for the dynamics of cutting process by Insperger and Stépán [29] and Insperger *et al.* [3]. In this paper, the generalization of this semi-discretization is shown and applied for demonstrative examples.

## 2. PRELIMINARIES

In this section, the main idea of semi-discretization is shown for a simple case. Let us consider the one-dimensional, second-order autonomous DDE with a discrete time delay

$$\ddot{x}(t) + c_0 x(t) = c_1 x(t - \tau) \quad (8)$$

The stability of the trivial solution  $x(t) \equiv 0$  of Equation (8) is known analytically. The stability chart shows the parameters  $c_0$  and  $c_1$  for which the system is stable. Although Equation (8) has infinite-dimensional phase space, its stability chart has the simple structure shown in Figure 1 [30]. The stability boundaries are lines with slope  $\pm 1$ . Grey coloured parameter domains refer to asymptotically stable systems.

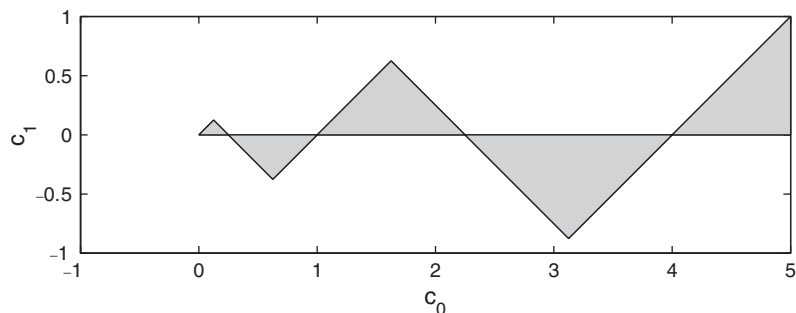
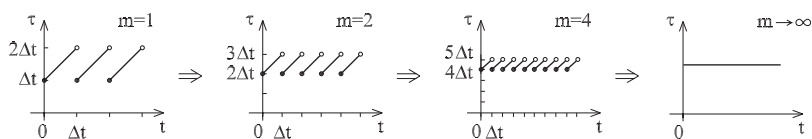
Figure 1. Stability chart for Equation (8) with  $\tau = 2\pi$ .

Figure 2. Time-dependent delay.

### 2.1. Basic idea of semi-discretization

Now, consider the intervals  $[t_i, t_{i+1})$  where  $t_{i+1} - t_i = \Delta t$ ,  $i = 0, 1, \dots$ , and the DDE

$$\ddot{x}(t) + c_0 x(t) = c_1 x(t_{i-m}), \quad t \in [t_i, t_{i+1}), \quad m \in \mathbb{Z}, \quad i = 0, 1, \dots \quad (9)$$

This equation for the case  $m = 1$  often comes up in control problems modelling the sampling effect [31]. In opposite to Equation (8), the time delay in Equation (9) is not constant, it is a piece-wise linear periodic function with period  $\Delta t$ , as it is shown in Figure 2. As the parameter  $m$  tends to infinity, the time delay tends to the constant value  $\tau$  if  $\Delta t = \tau / (m + \frac{1}{2})$  and Equation (9) approximates Equation (8).

Although Equation (9) is a non-autonomous DDE with infinite-dimensional phase space, its Poincaré map has a simple finite-dimensional representation since it can be solved in each time interval as an ODE (details will be explained in Section 3). The stability chart defined for various values of  $m$  can be seen in Figure 3 (stable parameter domains are denoted by grey colour). It shows, how the stability chart of Equation (9) approximates the chart of Equation (8) for increasing parameter  $m$ . For  $m = 10$ , the stability chart approximates the chart in Figure 1 with errors less than 1%. For the charts in Figure 3,  $\tau = 2\pi$ , consequently,  $\Delta t = 2\pi / (m + \frac{1}{2})$ .

For the case  $m = 1$ , the necessary and sufficient criteria for asymptotic stability can be given after a lengthy algebraic work (see Reference [32]) as

$$c_1 < c_0, \quad c_0 \neq \frac{k^2 \pi^2}{\Delta t^2} \quad (10)$$

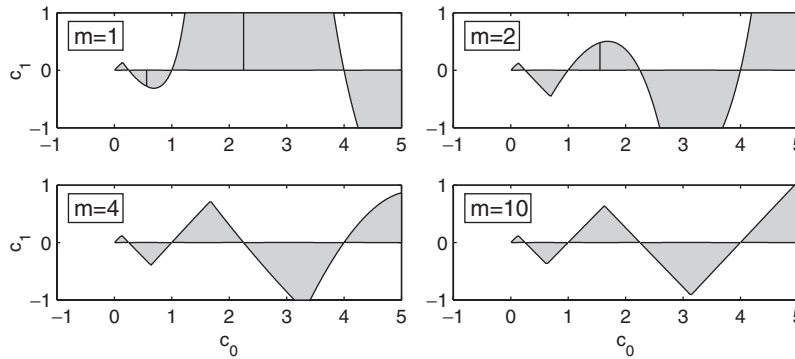


Figure 3. Stability chart for Equation (9) with  $\tau = 2\pi$ .

and

$$0 < c_1 < \frac{1 + 2 \cos(\sqrt{c_0} \Delta t)}{1 - \cos(\sqrt{c_0} \Delta t)} c_0 \quad \text{or} \quad 0 > c_1 > \frac{1 + 2 \cos(\sqrt{c_0} \Delta t)}{1 - \cos(\sqrt{c_0} \Delta t)} c_0 \tag{11}$$

where  $\Delta t = 4\pi/3$ . The formulae are more and more complicated for  $m \geq 2$ .

The point of the semi-discretization method is that, while the actual time domain terms are left in the original form, the delayed terms are approximated by piece-wise constant values, and are treated as constant excitations in ODEs. In Section 3, the generalization of the above introduced method will be shown. Before that, the full- and the semi-discretization are compared.

### 2.2. Full-discretization

The following question arises naturally: why do not we discretize all the actual time domain terms? The use of the interval division shown in Section 2.1 leads to the approximated derivatives of  $x(t)$

$$\dot{x}(t) \approx \frac{x_{i+1} - x_i}{\Delta t} \tag{12}$$

$$\ddot{x}(t) \approx \frac{x_{i+2} - 2x_{i+1} + x_i}{\Delta t^2} \tag{13}$$

where  $x_i = x(t_i)$ . Substitution into Equation (9) yields the recursive formula

$$x_{i+2} = \alpha_1 x_{i+1} + \alpha_2 x_i + \alpha_3 x_{i-m} \tag{14}$$

where  $\alpha_1 = 2$ ,  $\alpha_2 = -1 - c_0 \Delta t^2$  and  $\alpha_3 = c_1 \Delta t^2$ . This connection is described by the discrete map

$$\mathbf{y}_{i+1} = \mathbf{B}_i \mathbf{y}_i \tag{15}$$

where the  $m + 2$ -dimensional state vector is

$$\mathbf{y}_i = \text{col}(x_{i+1} \ x_i \ x_{i-1} \ \dots \ x_{i-m}) \tag{16}$$

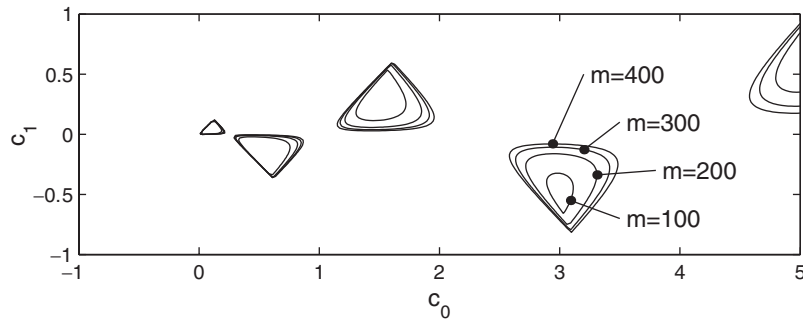


Figure 4. Stability charts constructed by full-discretization.

and the coefficient matrix has the form

$$\mathbf{B}_i = \begin{pmatrix} \alpha_1 & \alpha_2 & 0 & \dots & 0 & \alpha_3 \\ 1 & 0 & 0 & \dots & 0 & 0 \\ 0 & 1 & 0 & \dots & 0 & 0 \\ \vdots & \vdots & \vdots & \ddots & \vdots & \vdots \\ 0 & 0 & 0 & \dots & 0 & 0 \\ 0 & 0 & 0 & \dots & 1 & 0 \end{pmatrix} \quad (17)$$

The stability chart constructed by full discretization can be seen in Figure 4 for various approximation parameter values. Comparison of the charts in Figures 3 and 4 show, that the semi-discretization method is much more effective.

### 3. SEMI-DISCRETIZATION METHOD

The so-called semi-discretization is a well-known technique used for example, in the finite element analysis of solid bodies, or in computational fluid mechanics. The basic idea is, that the corresponding partial differential equation (PDE) is discretized along the spatial co-ordinates only, while the time co-ordinates are unchanged. From a dynamical systems viewpoint, the PDE has an infinite-dimensional state space, which is approximated by the finite-dimensional state space of a high-dimensional ODE.

The same idea can be used for any DDE, but its implementation is not trivial. The infinite-dimensional nature of the DDE is due to the presence of past effects, described by functions embedded also in the time domain, above the past interval  $[t - \sigma, t]$ , where  $\sigma$  denotes the length of the delay effect.

In this section, we will investigate the  $n$ -dimensional DDE

$$\dot{\mathbf{x}}(t) = \int_{-\sigma}^0 d_{\vartheta} \boldsymbol{\eta}(\vartheta, t) \mathbf{x}(t + \vartheta), \quad \boldsymbol{\eta}(\vartheta, t + T) = \boldsymbol{\eta}(\vartheta, t) \quad (18)$$

where the lower limit  $\sigma$  can also be infinity. The condition

$$\int_{-\infty}^0 e^{-v\vartheta} |d_{\vartheta} \eta_{jk}(\vartheta, t)| < \infty, \quad j, k = 1, 2, \dots, n, \quad v > 0, \quad t \in \mathbb{R} \quad (19)$$

is satisfied, where  $\eta_{jk}(\vartheta, t)$  are the elements of  $\boldsymbol{\eta}(\vartheta, t)$ . This condition means that the past effect decays at least exponentially in the past.

The integral in Equation (18) is a Stieltes one, i.e. it may contain discrete and continuous time delays, like

$$\int_{-\sigma}^0 d_{\vartheta} \boldsymbol{\eta}(\vartheta, t) \mathbf{x}(t + \vartheta) = \sum_{j=1}^r \mathbf{R}_j(t) \mathbf{x}(t - \tau_j) + \int_{-\sigma}^0 \mathbf{W}(\vartheta, t) \mathbf{x}(t + \vartheta) d\vartheta \quad (20)$$

where the number  $r$  of discrete time delays can also be infinity. Nevertheless, the discrete time delay can also be defined as

$$\mathbf{x}(t - \tau_j) = \int_{-\sigma}^0 w_j(\vartheta) \mathbf{x}(t + \vartheta) d\vartheta \quad (21)$$

where  $\sigma > \tau_j$  and the weight function is the Dirac distribution at  $-\tau_j$ :

$$w_j(\vartheta) = \delta(\vartheta + \tau_j) \quad (22)$$

This makes it possible to consider the discrete time delay as a special case of the continuous one. Thus we will investigate the DDE of the form

$$\dot{\mathbf{x}}(t) = \mathbf{A}(t) \mathbf{x}(t) + \int_{-\sigma}^0 \mathbf{W}(\vartheta, t) \mathbf{x}(t + \vartheta) d\vartheta \quad (23)$$

$$\mathbf{A}(t + T) = \mathbf{A}(t), \quad \mathbf{W}(\vartheta, t + T) = \mathbf{W}(\vartheta, t)$$

where  $\mathbf{W}(\vartheta, t)$  is now a weight distribution including such breaks like Dirac distribution, and dependence on the present state of  $\mathbf{x}(t)$  is determined by the matrix  $\mathbf{A}(t)$ . According to Equation (19), the condition for  $\mathbf{W}(\vartheta, t)$  reads

$$\int_{-\infty}^0 e^{-v\vartheta} |W_{jk}(\vartheta, t)| d\vartheta < \infty, \quad j, k = 1, 2, \dots, n, \quad v > 0, \quad t \in \mathbb{R} \quad (24)$$

Because of this condition, in approximations, the value of  $\sigma$  in Equation (23) can be considered as any large, but still finite value.

### 3.1. Structure of semi-discretization

One of the main steps of semi-discretization is the construction of the time intervals  $[t_i, t_{i+1})$  of length  $\Delta t$ ,  $i = 0, 1, \dots$ , so that the principal period can be expressed as  $T = k\Delta t$ ,  $k \in \mathbb{Z}$ .

There are three steps of approximations of the distribution matrix  $\mathbf{W}(\vartheta, t)$  in Equation (23).

1. Consider Equation (23) in the time intervals  $t \in [t_i, t_{i+1}]$ ,  $i = 0, 1, \dots$ . The time-dependent matrices  $\mathbf{A}(t)$  and  $\mathbf{W}(\vartheta, t)$  can be approximated with constant matrices  $\mathbf{A}_i$  and  $\mathbf{W}_i(\vartheta)$  for

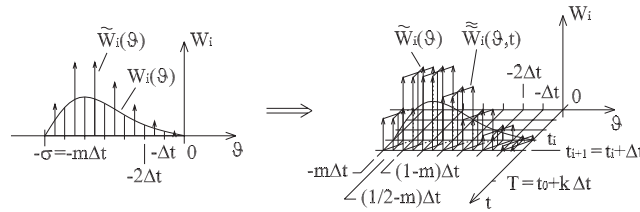


Figure 5. Approximation of the weight function.

each discretization interval

$$\mathbf{A}_i = \frac{1}{\Delta t} \int_{t_i}^{t_{i+1}} \mathbf{A}(t) dt \tag{25}$$

$$\mathbf{W}_i(\vartheta) = \frac{1}{\Delta t} \int_{t_i}^{t_{i+1}} \mathbf{W}(\vartheta, t) dt \tag{26}$$

that is  $\mathbf{A}_i$  and  $\mathbf{W}_i(\vartheta)$  are not time dependent any more. This step is equivalent to the piece-wise autonomous approximation of non-autonomous systems.

2. The continuous distribution matrix  $\mathbf{W}_i(\vartheta)$  can be approximated as a sum of shifted Dirac distributions

$$\tilde{\mathbf{W}}_i(\vartheta) = \sum_{j=1}^m \delta(\vartheta + (j - \frac{1}{2})\Delta t) \mathbf{W}_{i,j} \tag{27}$$

where the weights of the terms are

$$\mathbf{W}_{i,j} = \int_{-j\Delta t}^{(1-j)\Delta t} \mathbf{W}_i(\vartheta) d\vartheta \tag{28}$$

and  $m$  can also be infinity, similarly to  $\sigma$ . This step leads to a kind of piece-wise constant approximation of the delayed term.

3. Finally,  $\tilde{\mathbf{W}}_i(\vartheta)$  can be approximated with a time-dependent distribution for  $t \in [t_i, t_{i+1}]$

$$\tilde{\tilde{\mathbf{W}}}_i(\vartheta, t) = \tilde{\mathbf{W}}_i(\vartheta - \frac{1}{2}\Delta t + t) = \sum_{j=1}^m \delta(\vartheta + (j - 1)\Delta t + t) \mathbf{W}_{i,j} \tag{29}$$

This is a generalization of the approximation of discrete time delays shown in Figure 2.

The geometrical visualization of the approximation process can be seen in Figure 5.

The application of these approximations in Equation (23) results in a non-autonomous DDE which seems to be more complicated than the original DDE. However, the integral expression in Equation (23) can be approximated by a summation as follows:

$$\int_{-\sigma}^0 \mathbf{W}(\vartheta, t) \mathbf{x}(t + \vartheta) d\vartheta \approx \int_{-\sigma}^0 \tilde{\tilde{\mathbf{W}}}(\vartheta, t) \mathbf{x}(t + \vartheta) d\vartheta = \sum_{j=1}^m \mathbf{W}_{i,j} \mathbf{x}_{i-j+1} \tag{30}$$

where

$$\mathbf{x}_{i-j+1} = \mathbf{x}(t_i - (j-1)\Delta t), \quad i=0, 1, \dots, \quad j=0, 1, \dots, m \quad (31)$$

In spite of the fact, that the approximated system is a non-autonomous DDE, it can be defined as a series of autonomous ODEs with constant excitations in each discretization interval

$$\dot{\mathbf{x}}(t) = \mathbf{A}_i \mathbf{x}(t) + \sum_{j=1}^m \mathbf{W}_{i,j} \mathbf{x}_{i-j+1}, \quad t \in [t_i, t_{i+1}], \quad i=0, 1, \dots \quad (32)$$

In other words, Equation (23) is approximated now with a series of piece-wise autonomous ODEs.

Let us assume, that the matrix  $\mathbf{A}_i$  is invertible for all  $i$ . Then, the solution of Equation (32) takes the form

$$\mathbf{x}(t) = \exp(\mathbf{A}_i(t - t_i)) \mathbf{K}_i - \sum_{j=1}^m \mathbf{A}_i^{-1} \mathbf{W}_{i,j} \mathbf{x}_{i-j+1} \quad (33)$$

where the constant vector  $\mathbf{K}_i$  depends on the initial value  $\mathbf{x}(t_i) = \mathbf{x}_i$

$$\mathbf{K}_i = \mathbf{x}_i + \sum_{j=1}^m \mathbf{A}_i^{-1} \mathbf{W}_{i,j} \mathbf{x}_{i+1-j} \quad (34)$$

If the matrix  $\mathbf{A}_i$  is not invertible, then the solution can also be expressed, and the semi-discretization method can also be applied. However, we are not going into details on this issue.

Substitution of Equation (34) into Equation (33) and  $t = t_{i+1}$  yield

$$\mathbf{x}_{i+1} = \mathbf{M}_{i,0} \mathbf{x}_i + \sum_{j=1}^{m-1} \mathbf{M}_{i,j} \mathbf{x}_{i-j} \quad (35)$$

where the coefficient matrices are

$$\mathbf{M}_{i,0} = \exp(\mathbf{A}_i \Delta t) + (\exp(\mathbf{A}_i \Delta t) - \mathbf{I}) \mathbf{A}_i^{-1} \mathbf{W}_{i,1} \quad (36)$$

$$\mathbf{M}_{i,j} = (\exp(\mathbf{A}_i \Delta t) - \mathbf{I}) \mathbf{A}_i^{-1} \mathbf{W}_{i,j+1} \quad (37)$$

Equation (35) gives the connection between the states of the system at time instants  $t_i$  and  $t_{i+1}$ . This connection can be presented as a discrete map

$$\mathbf{y}_{i+1} = \mathbf{B}_i \mathbf{y}_i \quad (38)$$

where the  $mn$ -dimensional state vector is

$$\mathbf{y}_i = \text{col}(\mathbf{x}_i \quad \mathbf{x}_{i-1} \quad \dots \quad \mathbf{x}_{i-m+1}) \quad (39)$$

and the coefficient matrix is a hypermatrix of the form

$$\mathbf{B}_i = \begin{pmatrix} \mathbf{M}_{i,0} & \mathbf{M}_{i,1} & \mathbf{M}_{i,2} & \cdots & \mathbf{M}_{i,m-2} & \mathbf{M}_{i,m-1} \\ \mathbf{I} & \mathbf{0} & \mathbf{0} & \cdots & \mathbf{0} & \mathbf{0} \\ \mathbf{0} & \mathbf{I} & \mathbf{0} & \cdots & \mathbf{0} & \mathbf{0} \\ \vdots & \vdots & \vdots & \ddots & \vdots & \vdots \\ \mathbf{0} & \mathbf{0} & \mathbf{0} & \cdots & \mathbf{0} & \mathbf{0} \\ \mathbf{0} & \mathbf{0} & \mathbf{0} & \cdots & \mathbf{I} & \mathbf{0} \end{pmatrix} \quad (40)$$

The next step is to determine the transition matrix  $\Phi$  over the principal period  $T = k\Delta t$ . This serves a finite-dimensional approximation of the monodromy operator in the infinite-dimensional version of the Floquet theory [23]. The transition matrix gives the connection between  $\mathbf{y}_0$  and  $\mathbf{y}_k$  in the form

$$\mathbf{y}_k = \Phi \mathbf{y}_0 \quad (41)$$

where  $\Phi$  is given by coupling the solutions

$$\Phi = \mathbf{B}_{k-1} \mathbf{B}_{k-2} \cdots \mathbf{B}_1 \mathbf{B}_0 \quad (42)$$

This transition matrix is a finite-dimensional approximation of the  $\mathbf{U}(T)$  operator of Equation (23). Now, the stability investigation of Equation (32) is reduced to the problem, whether the eigenvalues of  $\Phi$  are in modulus less than 1 [33]. Any standard or advanced numerical algorithm [34] can be used for this last step.

### 3.2. Convergence of semi-discretization

The convergence of the method can be seen by refining the interval division, e.g. by decreasing  $\Delta t$  and increasing  $m$ . The approximation defined by Equation (30) satisfies

$$\lim_{\Delta t \rightarrow 0} \int_{-\sigma}^0 \tilde{\mathbf{W}}(\vartheta, t) \mathbf{x}(t + \vartheta) d\vartheta = \lim_{\Delta t \rightarrow 0} \sum_{j=1}^m \mathbf{W}_{i,j} \mathbf{x}_{t-j+1} = \int_{-\sigma}^0 \mathbf{W}(\vartheta, t) \mathbf{x}(t + \vartheta) d\vartheta \quad (43)$$

since it is a rectangular sum approximation of integral expressions according to the classical definition of the Riemann integral.

Let us denote the characteristic multipliers of the original Equation (18) by  $\mu_j$ ,  $j = 1, 2, \dots$ , and the characteristic multipliers of the approximating Equation (41) by  $\tilde{\mu}_j$ ,  $j = 1, 2, \dots, mn$ .

For any small  $\varepsilon > 0$ , there exists an integer  $M(\varepsilon)$ , so that for every  $m > M(\varepsilon)$ , the set  $\bigcup_{j=1}^{mn} S_{\tilde{\mu}_j, \varepsilon}$  contains exactly  $mn$  number of characteristic multipliers  $\mu_j$  of Equation (18), and all the other characteristic multipliers of Equation (18) are in modulus less than  $\varepsilon$ .

Thus, if all the characteristic multipliers of Equation (41) are in modulus less than 1, then choosing  $\varepsilon = \frac{1}{2}(1 - \max_j |\tilde{\mu}_j|)$ , the finite approximation number  $M(\varepsilon)$  exists, and if  $m > M(\varepsilon)$  fulfils, then the discretized and the original system has the same stability properties (see Figure 6 with  $nm = 3$ ). A rigorous proof of the above statement can be constructed with the methods presented by Farkas and Stépán [35] which use the continuous dependence of the eigenvalues on the system parameters.

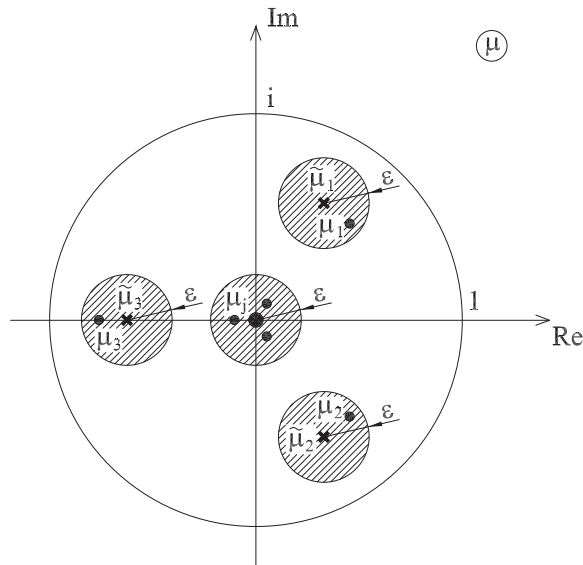


Figure 6. Eigenvalue localization.

Clearly, the semi-discretization does not preserve the solutions of the original system. It preserves, however, their exponential stability if the semi-discretization is fine enough in the sense presented above. It does not preserve stability in critical linear cases which do not resist non-linear perturbations.

#### 4. EXAMPLES

One-dimensional, higher-order systems can be investigated by transforming the system into the form of Equation (23) according to the Cauchy transformation, and then using the semi-discretization method. In some special cases of higher-order systems, the direct semi-discretization leads to a lower-dimensional approximation than the semi-discretization of the Cauchy-transformed systems. This is the case, for example, when the Mathieu equation

$$\ddot{x}(t) + b_0\dot{x}(t) + c_0(t)x(t) = c_1 \int_{-1}^0 w(\vartheta)x(t + \vartheta) d\vartheta, \quad c_0(t) = c_{0\delta} + c_{0e} \cos(2\pi t/T) \quad (44)$$

is investigated with continuous time delay of maximum length 1. Let the time interval division be defined as in Section 3.1. In the interval  $t \in [t_i, t_{i+1})$ , Equation (44) can be approximated as

$$\ddot{x}(t) + b_0\dot{x}(t) + c_{0,i}x(t) = c_1 \sum_{j=1}^m w_j x_{i-j+1} \quad (45)$$

where

$$c_{0,i} = \frac{1}{\Delta t} \int_{t_i}^{t_{i+1}} c_0(t) dt \approx c_0(t_i + \Delta t/2) \quad (46)$$

$$w_j = \int_{-j\Delta t}^{(1-j)\Delta t} w(\vartheta) d\vartheta \approx \Delta t w((1/2 - j)\Delta t) \quad (47)$$

For the initial conditions  $x(t_i) = x_i$ ,  $\dot{x}(t_i) = \dot{x}_i$ , the solution and its derivative at time  $t_{i+1}$  can be determined

$$x_{i+1} = x(t_{i+1}) = a_{0,0}x_i + a_{0,1}\dot{x}_i + \sum_{h=1}^{m-1} b_{0,h}x_{i-h} \quad (48)$$

$$\dot{x}_{i+1} = \dot{x}(t_{i+1}) = a_{1,0}x_i + a_{1,1}\dot{x}_i + \sum_{h=1}^{m-1} b_{1,h}x_{i-h} \quad (49)$$

where

$$a_{0,0} = \kappa_{1,0} \exp(\lambda_1 \Delta t) + \kappa_{2,0} \exp(\lambda_2 \Delta t) + c_1 w_1 / c_{0,i}$$

$$a_{0,1} = \kappa_{1,1} \exp(\lambda_1 \Delta t) + \kappa_{2,1} \exp(\lambda_2 \Delta t)$$

$$a_{1,0} = \kappa_{1,0} \lambda_1 \exp(\lambda_1 \Delta t) + \kappa_{2,0} \lambda_2 \exp(\lambda_2 \Delta t)$$

$$a_{1,1} = \kappa_{1,1} \lambda_1 \exp(\lambda_1 \Delta t) + \kappa_{2,1} \lambda_2 \exp(\lambda_2 \Delta t)$$

$$b_{0,h} = \sigma_{1,h} \exp(\lambda_1 \Delta t) + \sigma_{2,h} \exp(\lambda_2 \Delta t) + c_1 w_{h+1} / c_{0,i}, \quad h = 1, 2, \dots, m-1$$

$$b_{1,h} = \sigma_{1,h} \lambda_1 \exp(\lambda_1 \Delta t) + \sigma_{2,h} \lambda_2 \exp(\lambda_2 \Delta t), \quad h = 1, 2, \dots, m-1$$

and

$$\kappa_{1,0} = \frac{\lambda_2(1 - c_1 w_1 / c_{0,i})}{\lambda_2 - \lambda_1}, \quad \kappa_{1,1} = \frac{-1}{\lambda_2 - \lambda_1}, \quad \sigma_{1,j} = \frac{-\lambda_2 c_1 w_{j+1} / c_{0,i}}{\lambda_2 - \lambda_1}$$

$$\kappa_{2,0} = \frac{-\lambda_1}{\lambda_2} \kappa_{1,0}, \quad \kappa_{2,1} = -\kappa_{1,1}, \quad \sigma_{2,j} = \frac{-\lambda_1}{\lambda_2} \sigma_{1,j}$$

$$\lambda_{1,2} = \frac{-b_0 \pm \sqrt{b_0^2 - 4c_{0,i}}}{2}$$

Equations (48) and (49) define the discrete map

$$\mathbf{y}_{i+1} = \mathbf{B}_i \mathbf{y}_i \quad (50)$$

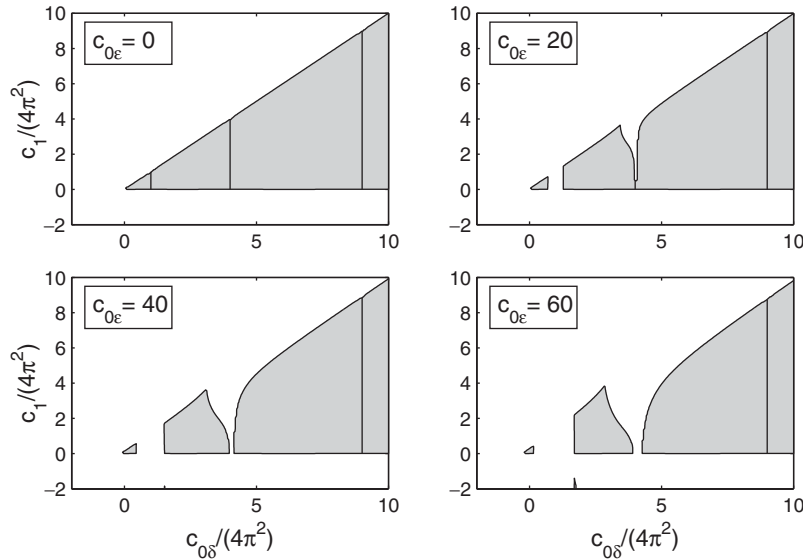


Figure 7. Stability chart for Equation (44) for  $w(\vartheta) \equiv 1$ ,  $b_0 = 0$ ,  $T = \frac{1}{2}$ .

where the  $m + 1$ -dimensional state vector is

$$y_i = \text{col}(\dot{x}_i \ x_i \ x_{i-1} \ \dots \ x_{i-m+1}) \tag{51}$$

and the coefficient matrix has the form

$$B_i = \begin{pmatrix} a_{1,1} & a_{1,0} & b_{1,1} & b_{1,2} & \dots & b_{1,m-2} & b_{1,m-1} \\ a_{0,1} & a_{0,0} & b_{0,1} & b_{0,2} & \dots & b_{0,m-2} & b_{0,m-1} \\ 0 & 1 & 0 & 0 & \dots & 0 & 0 \\ 0 & 0 & 1 & 0 & \dots & 0 & 0 \\ \vdots & \vdots & \vdots & \vdots & \ddots & \vdots & \vdots \\ 0 & 0 & 0 & 0 & \dots & 0 & 0 \\ 0 & 0 & 0 & 0 & \dots & 1 & 0 \end{pmatrix} \tag{52}$$

Now, the transition matrix can be given according to Equation (42), and the stability can be determined by simple eigenvalue analysis.

Three types of weight functions are considered, all of them are taken from the book of Stépán [2]. The stability charts are shown in Figures 7, 8 and 9 for principal period  $T = \frac{1}{2}$  and coefficients  $b_0 = 0$ ,  $c_{0ε} = 0, 20, 40, 60$ . The charts for the autonomous case, when  $c_{0ε} = 0$ , were constructed in closed form in Reference [2]. These cases can be used for checking the accuracy of the method. The approximation number  $m = 20$ , that is a 21-dimensional discrete map approximation of the infinite-dimensional Equation (44) results stability boundaries with errors less than 1% in the parameter domain considered here.

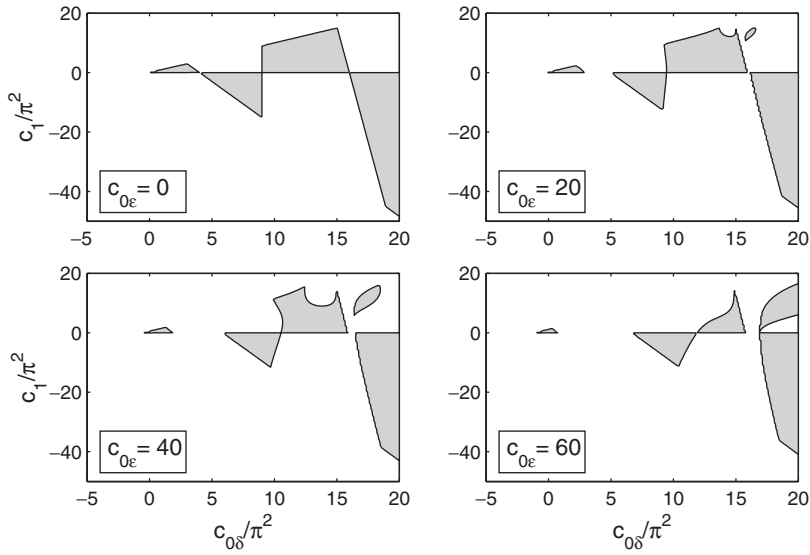


Figure 8. Stability chart for Equation (44) for  $w(\vartheta) = -(\pi/2) \sin(\pi\vartheta)$ ,  $b_0 = 0$ ,  $T = \frac{1}{2}$ .

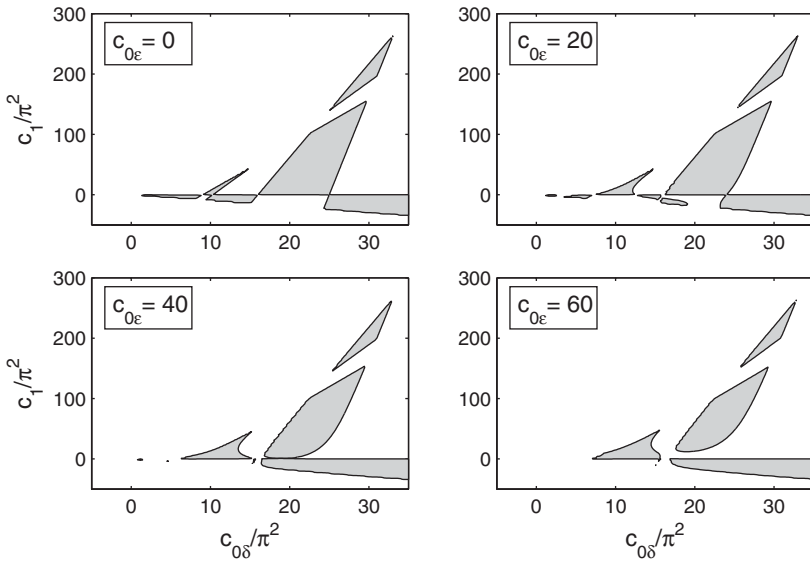


Figure 9. Stability chart for Equation (44) for  $w(\vartheta) = (\pi/2) \sin(\pi\vartheta) + (13\pi/77) \sin(2\pi\vartheta)$ ,  $b_0 = 0$ ,  $T = \frac{1}{2}$ .

As an even more complex problem, study the equation

$$\ddot{x}(t) + (6 + c_{0\epsilon} \cos 2\pi t)x(t) = x(t - \tau_1) + x(t - \tau_2) \tag{53}$$

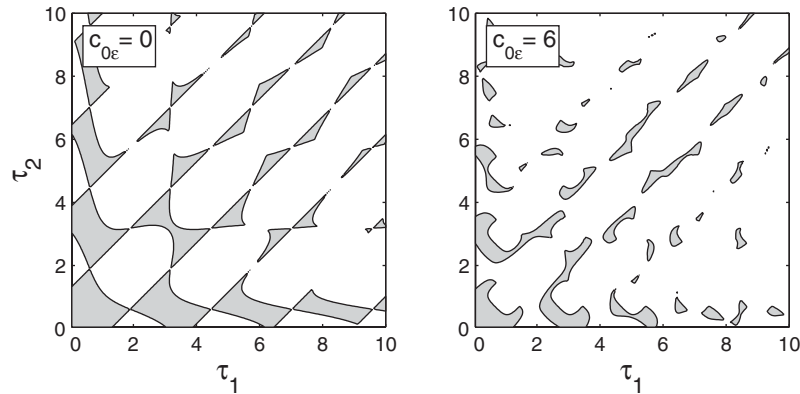


Figure 10. Stability chart for Equation (53).

In this case  $T=1$ ,  $b_0=0$ ,  $c_{0\delta}=6$ ,  $c_1=1$  and  $w(\vartheta)=\delta(\vartheta+\tau_1)+\delta(\vartheta+\tau_2)$  in Equation (44). For the cases  $c_{0\epsilon}=0$  and 6, the stability charts in the parameter plane of time delays  $\tau_1$  and  $\tau_2$  can be seen in Figure 10. The analysis of the autonomous two-delay system ( $c_{0\epsilon}=0$ ) can also be found in Reference [2].

The stability charts were made by point by point investigation of the parameter domain. The stability boundaries were determined by refining the resolution using the algorithm of Szabó and Lóránt [36]. The stable parameter domains are denoted by grey colour.

## 5. CONCLUSIONS

Time periodic delay models are rarely used by engineers due to the difficulties in the analysis of the corresponding differential equations even in the linear case. An efficient method was shown for the stability investigation of linear periodic DDEs. The semi-discretization method was compared to the full-discretization in the time domain. The method was applied for the delayed Mathieu equation with continuous delay and two discrete delays, and a range of intriguing stability charts were plotted. These charts can easily be transformed further into the domains of physical parameters for problems like regenerative machine tool vibrations, remote force reflective manipulation, or human machine systems.

## ACKNOWLEDGEMENTS

This research was supported by the Hungarian National Science Foundation under Grant No. OTKA T030762/99 and by COST Action P4.

## REFERENCES

1. Stépán G. Delay-differential equation models for machine tool chatter. In *Dynamics and Chaos in Manufacturing Processes*, Moon FC (ed.), Wiley: New York, 1998; 165–192.
2. Stépán G. *Retarded Dynamical Systems*. Longman: Harlow, 1989.

3. Insperger T, Stépán G, Namachchivaya S. Comparison of the dynamics of low immersion milling and cutting with varying spindle speed. In *Proceedings of the ASME 2001 Design Engineering Technical Conferences*, Pittsburgh, Pennsylvania, 2001, Paper no. DETC2001/VIB-21616 (CD-ROM).
4. Insperger T, Stépán G. Stability of the milling process. *Periodica Polytechnica* 2000; **44**(1):47–57.
5. Insperger T, Stépán G. Remote control of periodic robot motion. In *Proceedings of 13th CISM-IFTOMM Symposium on Theory and Practice of Robots and Manipulators*, Zakopane, Springer: Wien, 2000; 197–203.
6. Routh EJ. *A Treatise on the Stability of a Given State of Motion*. Macmillan, London, 1877.
7. Hurwitz A. Über die bedingungen unter welchen eine gleichung nur wurzeln mit negativen reellen teilen besitzt. *Mathematische Annalen* 1895; **46**:74–81.
8. Floquet MG. Équations différentielles linéaires à coefficients périodiques. *Annales Scientifiques de l'École Normale Supérieure* 1883; **12**:47–89.
9. Hill GW. On the part of the motion of the lunar perigee which is a function of the mean motions of the Sun and Moon. *Acta Mathematica* 1886; **8**:1–36.
10. D'Agelo H. *Linear Time-varying System: Analysis and Synthesis*. Allyn and Bacon: Boston, 1970.
11. Nayfeh AH, Mook DT. *Nonlinear Oscillations*. Wiley: New York, 1979.
12. Sinha SC, Wu DH. An efficient computational scheme for the analysis of periodic systems. *Journal of Sound and Vibration* 1991; **151**:91–117.
13. van der Pol F, Strutt MJO. On the stability of the solutions of Mathieu's equation. *Philosophical Magazine, and Journal of Science* 1928; **5**:18–38.
14. Hale JK. *Theory of Functional Differential Equations*. Springer: New York, 1977.
15. Hale JK, Lunel SMV. *Introduction to Functional Differential Equations*. Springer: New York, 1993.
16. Diekmann O, van Gils SA, Lunel SMV, Walther H-O. *Delay Equations*. Springer: New York, 1995.
17. Bellman R, Cooke K. *Differential-Difference Equations*. Academic Press: New York, 1963.
18. Bhatt SJ, Hsu CS. Stability criteria for second-order dynamical systems with time lag. *Journal of Applied Mechanics* (ASME) 1966; **33E**(1):113–118.
19. Neimark Ju I. D-subdivision and spaces of quasi-polynomials. *Prikladnaja Matematika i Mechanika* 1949; **13**(4):349–380 (in Russian).
20. Pontryagin LS. On the zeros of some elementary transcendental functions. *Izvestiya Akademiyi Nauk SSSR* 1942; **6**(3):115–134 (in Russian).
21. Kolmanovskii VB, Nosov VR. *Stability of Functional Differential Equations*. Academic Press: London, 1986.
22. Hassard BD. Counting roots of the characteristic equation for linear delay-differential systems. *Journal of Differential Equations* 1997; **136**:222–235.
23. Farkas M. *Periodic Motions*. Springer: New York, 1994.
24. Balachandran B. Non-linear dynamics of milling process. *Philosophical Transactions of the Royal Society* 2001; **359**:793–820.
25. Davies MA, Pratt JR, Dutterer B, Burns TJ. Stability prediction for low radial immersion milling. *Journal of Manufacturing Science and Engineering* (ASME) 2002; **124**(2):217–225.
26. Bayly PV, Halley JE, Mann BP, Davies MA. Stability of interrupted cutting by temporal finite element analysis. In *Proceedings of the ASME 2001 Design Engineering Technical Conferences*, Pittsburgh, Pennsylvania, 2001, Paper no. DETC2001/VIB-21581 (CD-ROM).
27. Seagalman DJ, Butcher EA. Suppression of regenerative chatter via impedance modulation. *Journal of Vibration and Control* 2000; **6**:243–256.
28. Insperger T, Stépán G. Stability chart for the delayed Mathieu equation. *Proceedings of The Royal Society, Mathematical Physical and Engineering Sciences* 2002, vol 458, in press.
29. Insperger T, Stépán G. Semi-discretization of delayed dynamical systems. In *Proceedings of the ASME 2001 Design Engineering Technical Conferences*, Pittsburgh, Pennsylvania, 2001, Paper no. DETC2001/VIB-21446 (CD-ROM).
30. Hsu CS, Bhatt SJ. Stability charts for second-order dynamical systems with time lag. *Journal of Applied Mechanics* (ASME) 1966; **33E**(1):119–124.
31. Stépán G. Vibrations of machines subjected to digital force control. *International Journal of Solids and Structures* 2001; **38**(10–13):2149–2159.
32. Stépán G. Varying delay and stability in dynamical systems. *Zeitschrift für Angewandte Mathematik und Mechanik* 1991; **71**(4):154–156.
33. Lakshmikantham V, Trigiante D. *Theory of Difference Equations, Numerical Methods and Applications*. Academic Press: London, 1988.
34. Bauchau OA, Nikishkov YG. An implicit Floquet analysis for rotorcraft stability evaluation. *Journal of the American Helicopter Society* 2001; **46**:200–209.
35. Farkas M, Stépán G. On perturbation of the kernel in infinite delay systems. *Zeitschrift für Angewandte Mathematik und Mechanik* 1992; **72**(2):153–156.
36. Szabó Zs, Lóránt G. Parametric excitation of a single railway wheelset. *Vehicle System Dynamics* 2000; **33**(1):49–55.